Hydrodynamic Simulation of Periodic Cycled Plate Columns

A mathematical model of the hydrodynamic processes occurring in a periodic cycled plate column is developed and experimentally confirmed. The model is applied to the prediction of the holdup distribution and the investigation of hydrodynamic problems. An effective manifold arrangement is proposed to minimize the uneven liquid draining encountered in previous experimental studies.

M. F. THOMPSON and I. A. FURZER

Department of Chemical Engineering
The University of Sydney
NSW 2006, Australia

SCOPE

The operation of a plate column contacting vapor and liquid in a periodic cycled mode is essentially an unsteady-state process. During the vapor flow period (VFP), the liquid on the sieve plates is supported by the passage of vapor up the column, and mass transfer occurs. The vapor is then bypassed from the column during the liquid flow period (LFP) allowing the liquid to drain to the plate below.

Theoretical studies by Sommerfeld et al. (1966), Horn (1967), and Furzer (1973) showed that the efficiency of a periodic cycled column was twice that of conventional columns. However, experimental studies by Duffy (1976) and Szonyi (1981) failed to achieve the theoretical efficiencies in multiple-plate columns, even though they obtained good correlations in single-plate experiments. The poor efficiencies of the multiple-plate columns were attributed to hydrodynamic problems occurring during the LFP. Lags in the pressure transients resulted in uneven liquid draining and deviations from the assumption of liquid plug flow in the theoretical treatment.

The objective of this study is to develop an experimentally confirmed hydrodynamic model of a periodic cycled column. The model will be used to investigate the effect of column parameters and manifold design in minimizing the hydrodynamic problems encountered by previous workers.

CONCLUSIONS AND SIGNIFICANCE

A hydrodynamic model of a periodic cycled column, based on material and energy balances, was developed to investigate the problems associated with the LFP. The pressure responses of the vapor spaces, which directly control the liquid flow, were subject to delays from several sources. The model simulations clearly showed that the flashing of the liquid holdup during the initial stages of the LFP constituted the most significant delay in nonisothermal columns. The performance of various vapor venting arrangements in reducing this delay was evaluated using the hydrodynamic model. A manifold connecting each vapor space with increasing branch areas down the column was the most effective arrangement. A solenoid-operated isolation valve at the manifold outlet and check valves on the branches prevented vapor losses during the VFP. The simulations showed the design parameters of plate free area, and branch diameter had the largest effect on the plate holdups.

Experiments were conducted on a four-plate 610 mm diameter column, operated with an air/water system, to confirm the validity of the isothermal hydrodynamic model. The simulations were in close agreement with both the dynamic pressure responses and the pseudosteady-state holdup distributions obtained experimentally over a range of conditions.

The results of the investigations confirmed that the model could capably describe the hydrodynamic processes occurring in a periodic cycled column. In addition to its application to minimizing the hydrodynamic problems, the model provides a means of predicting the holdup distribution, based on column design parameters. This information, essential to the mass transfer calculation, has not previously been available at the design stage.

INTRODUCTION

The hydrodynamic modeling of periodic cycled columns has concentrated on the liquid flow period (LFP), as the vapor flow period (VFP) is well understood from conventional distillation studies. The models can be classified into two groups, the experimentally based parameter estimation mixing models and the dynamic models.

The mixing models attempt to quantify the deviations from plug flow during the LFP to describe the differences between the experimental and theoretical efficiencies. Horn and May (1968) simulated each plate with a series of perfectly mixed tanks. The column performance improved as the number of tanks increased, corresponding to an approach to plug flow. Gerster and Scull (1970) proposed a model consisting of a plug flow section, describing the liquid falling to the plate below, and a perfectly mixed fraction of liquid on the plate. Furzer and Duffy (1976) introduced a 2S model which consisted of two parameters representing the fractions of the liquid holdup that drops to the next two plates respectively. This model allowed the calculation of plate holdups once the parameters had been determined. In all the mixing models, the parameters must be evaluated from experiments on the particular column.

The dynamic model consists of a series of differential equations based on the conservation laws. These equations are solved in conjunction with plate performance equations describing instantaneous liquid and vapor flows within the column. The first reported study of a dynamic model was made by Wade et al. (1969). Their model, consisting of an overall and component molar balance and an energy balance, for each plate, was solved using Euler's method. Their simulations predicted a dead time before successive plates commenced draining, and they reported that free area adjustments did not stabilize the flow profiles. Wade et al. assumed that the pressure above a plate was equal to the vapor pressure of the liquid and that ideal thermodynamic behavior occurred. They did not state the system used in their simulations.

Larsen and Kümmel (1979) presented solutions for a dynamic model of a one-component n-heptane system. They utilized a more complex plate performance model and included a differential equation for the vapor space molar balance to accommodate the effects of liquid flashing. Larsen and Kümmel (1979) assumed a constant vapor volume, and equal liquid and vapor temperatures, using a stiff differential equation integration algorithm to obtain a solution. They showed that omitting the energy balance had a significant effect on the liquid and vapor flow profiles, and they examined the liquid holdup transients over a number of cycles. The dynamic modeling studies of Wade et al. (1969) and Larsen and Kümmel (1979) were of a general nature without any experimental confirmation of their results.

THEORY

Dry Column Model

The dynamic pressure responses below each plate in a periodic cycled column have a sisngificant effect on the hydrodynamic performance of the column. The dry column model was developed to investigate the effect of the column dynamics on the pressure responses. The vapor in the column was assumed to behave as an ideal gas with isothermal and incompressible flow. The resistances to vapor flow were considered to be independent of Reynolds number, and the dynamics of the butterfly valve in the vapor supply line were assumed to have a negligible effect upon the pressure response. A schematic diagram of the dry column fitted with a manifold to assist vapor venting is shown in Figure 1.

A molar balance is performed on the volume, G_n under plate n

$$\frac{dN_n}{dt} = V_{n+1} - V_n - W_{b,n} \tag{1}$$

The molar vapor flow through the plates, V_n and in the manifold branches, $W_{b,n}$ is described by orifice equations of the form

$$V_n = \frac{A_c}{M_{W,V}}\left(\frac{2\rho_V}{k_{V,n}}\right)^{1/2}(P_n - P_{n-1})^{1/2} \tag{2}$$

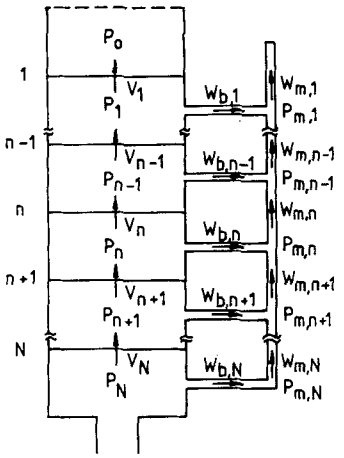

Figure 1. Diagram of dry column with a manifold.

The manifold is treated as a flow network with nodes at the trees as shown in Figure 1. The molar vapor holdup, N_n as described by the ideal gas equation of state,

$$N_n = \frac{G_n P_n}{RT} \tag{3}$$

is combined with Eqs. 1 and 2. The resultant series of differential equations are nondimensionalized by defining P_n^* as the ratio of actual gauge pressure to maximum gauge pressure under plate n.

$$P_n^* = \frac{P_n - P_a}{n\overline{\Delta P_d}} \tag{4}$$

The pressure responses are described by

$$\frac{dP_n^*}{dt^*} = \frac{1}{G_n^*}\left\{\left[\left(\frac{n+1}{n^2}\right)P_{n+1}^* - \left(\frac{1}{n}\right)P_n^*\right]^{1/2} - \left[\left(\frac{1}{n}\right)P_n^* - \left(\frac{n-1}{n^2}\right)P_{n-1}^*\right]^{1/2} - \left[\frac{\alpha_n}{\beta_n}\left(\frac{1}{n}\right)(P_n^* - P_{m,n}^*)\right]^{1/2}\right\} \quad \text{for } n = 1, \ldots, N \tag{5}$$

where

$$\alpha_n = \left(\frac{k_{V,n}}{k_{b,n}}\right)^{1/2} \tag{6}$$

and

$$\beta_n = \frac{A_c}{A_{b,n}} \tag{7}$$

The dimensionless time t^* is defined by

$$T^* = \frac{RTA_c}{M_{W,V}G_T}\left(\frac{2\rho_V}{k_{V,n}\overline{\Delta P_d}}\right)^{1/2} t \tag{8}$$

and the volume between the plates is nondimensionalized with respect to a standard volume, G_T

$$G_n^* = \frac{G_n}{G_T} \tag{9}$$

The set of differential equations (Eq. 5) were solved using the Numerical Algorithm Group (NAG) (1981), variable step length, Runge-Kutta-Merson (RKM) routine on a CYBER 140-730 computer. The manifold network equations were solved by iterative techniques for each evaluation of the derivatives. The dynamics

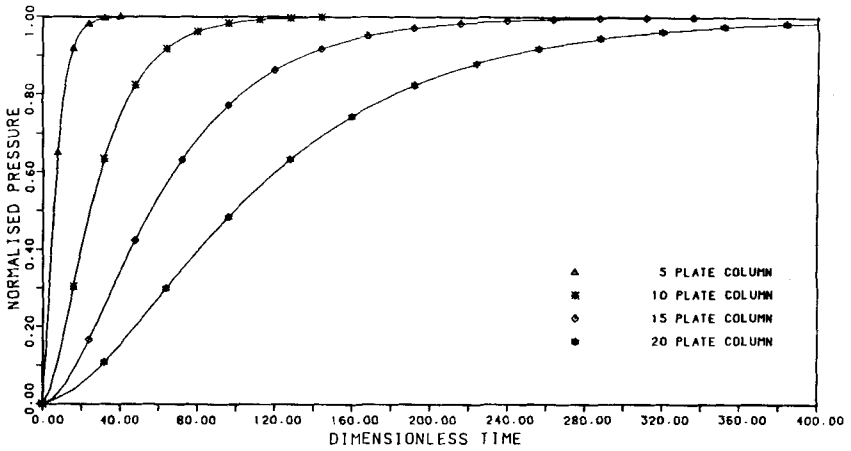

Figure 2. Effect of number of plates on top plate positive pressure response in a dry column.

of the butterfly valve in the vapor supply line were assumed to have a negligible effect upon the pressure responses. For the increasing pressure positive response, the vapor space below the bottom plate instantaneously attained its steady state condition. The negative responses were obtained with no vapor flow into the column.

The positive and negative pressure responses below the top plate in the dry column simulations are shown in Figures 2 and 3. For an air system in a 600 mm diameter column with a 0.5 kPa plate pressure drop, 50 dimensionless time units correspond to 0.15 s. The time required for a five-plate column to approach steady state after a positive response was less than 0.2 s, while the negative response was complete in less than 0.1 s. These extremely rapid responses show the delays in the pressure transients that were not due to the dynamics of the column.

Hydrodynamic Model

The hydrodynamic model was developed to investigate the influence of the liquid holdups upon the pressure responses and liquid draining characteristics in a periodic cycled column. The hydrodynamic model was based on the dry column model with the inclusion of a liquid holdup on each plate. It was assumed that no mass transfer occurred between the vapor and liquid phases and that the weeping and entrainment during the VFP was negligible. The hydrodynamic model was developed for a column fitted with time delay plates (TDP), to reduce liquid mixing during the LFP, and with vents to atmosphere under each plate.

The molar balance in the vapor space below plate n is given by Eq. 1. The volume of the vapor space, G_n is dependent on the holdup h_{n+1} on the plate below and the amount of liquid delayed in the TDP, $M_{D,n}$

$$G_n = A_c(H_{e,n} - h_{n+1}) - \frac{M_{D,n}M_{W,L}}{\rho_L} \tag{10}$$

The time derivative of the ideal gas, Eq. 2, becomes

$$\frac{dN_n}{dt} = \frac{1}{RT}\left(G_n\frac{dP_n}{dt} + P_n\frac{dG_n}{dt}\right) \tag{11}$$

The resultant differential equations describing the pressure response are

$$\frac{dP_n}{dt} = \frac{RT[V_{n+1} - V_n - W_{b,n}] + P_n\left[A_c\frac{dh_{n+1}}{dt} + \left(\frac{M_{W,L}}{\rho_L}\right)\frac{dM_{D,n}}{dt}\right]}{A_c(H_{e,n} - h_{n+1}) - \left(\frac{M_{W,L}}{\rho_L}\right)M_{D,n}} \quad \text{for } n = 1, \ldots, N \tag{12}$$

A molar balance around the liquid on plate n gives

$$\frac{dh_n}{dt} = \frac{M_{W,L}}{A_c\rho_L}(Q_{D,n-1} - L_n) \qquad \text{for } n = 1, \ldots, N+1 \tag{13}$$

where $Q_{D,n-1}$ is the molar flow of liquid from the TDP mixing with the liquid on plate n. A simple model of the TDP is obtained from a molar liquid balance over the vapor space.

$$\frac{dM_{D,n}}{dt} = L_n - Q_{D,n} \qquad \text{for } n = 1, \ldots, N-1 \tag{14}$$

The delayed liquid molar flow, $Q_{D,n}$ is a function of the molar holdup in the TDP combined with a time delay.

The liquid and vapor molar flows through the plates are determined from the simple plate performance model used by Wade et al (1969). The pressure difference across the dry plate, $\Delta P_{d,n}$ dictates whether liquid or vapor flow occurs.

$$\Delta P_{d,n} = P_n - P_{n-1} - \rho_L g h_n \tag{15}$$

Vapor Molar Flows

$$V_n = \frac{A_c}{M_{W,V}}\left(\frac{2\rho_V\Delta P_{d,n}}{k_V}\right)^{1/2} \text{ for } \Delta P_{d,n} > 0.0$$
$$V_n = 0.0 \text{ for } \Delta P_{d,n} \leq 0.0 \tag{16}$$

Liquid Molar Flows

$$L_n = \frac{A_c}{M_{W,L}}\left(\frac{-2\rho_L\Delta P_{d,n}}{k_L}\right)^{1/2} \text{for } \Delta P_{d,n} < 0.0$$
$$L_n = 0.0 \quad \text{for } \Delta P_{d,n} \geq 0.0 \tag{17}$$

where k_V and k_L are the plate resistances to vapor and liquid flow, based on the column area, A_c.

The hydrodynamic model for an N-plate column—Eqs. 12, 13, and 14—requires the solution of $3N$ differential equations. Thompson and Furzer (1983) compared the performance of the RKM method, the predictor corrector Adams procedure, and the Gear method for stiff differential equations for solving the hydrodynamic model equations. The RKM method was the most

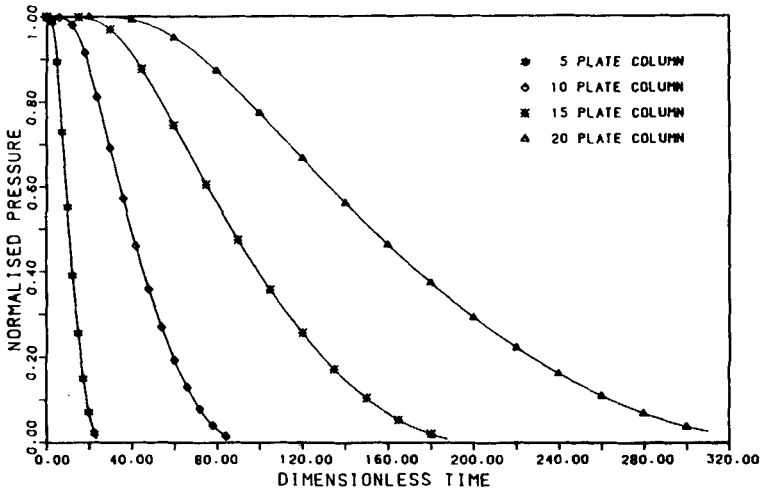

Figure 3. Effect of number of plates on top plate negative pressure response in a dry column.

efficient during the LFP and the initial stages of the VFP, when both pressure and holdup derivatives were of a similar magnitude. The Gear algorithm was used when the equations became stiff once the rapid pressure transients at the start of the VFP were complete. The routines were available from the NAG (1981) subroutine library on a CYBER 170-730 computer. The initial conditions were obtained at the end of the VFP when the pressures and plate holdups had attained constant values. The initial conditions were specified in terms of either the pressure profile or holdup distribution, which were related by Eqs. 15 and 16.

The computing time was reduced by scaling the pressure terms to kilopascals, reducing the derivatives to a similar magnitude during the LFP. A number of points of solution instability resulted in excessive computational times. As the plate pressure drop ratio ($\Delta P_d/\rho_L gh$) approached unity in unvented columns, large changes in liquid and vapor flow occurred with small changes in pressure, producing an unstable solution. This was overcome by introducing simultaneous vapor and liquid flow when the pressure drop ratio approached unity. In vented columns, the continuous flow of vapor through the vent insured that the pressure drop ratio did not remain near unity. Complete drainage of the plates resulted in further instabilities as plate holdups tended to become negative. A minimum plate holdup of 0.04 mm of liquid was set, and once this was attained the liquid reaching the plate was assumed to pass directly through it and downflow of vapor could occur. A minimum pressure difference of 0.5 Pa between the plates, under these conditions, prevented the instabilities caused by frequent changes in vapor flow direction due to the small driving forces.

A pseudosteady-state (PSS) solution to the hydrodynamic model was achieved when the holdups at the end of the VFP, $h_n(t_v)$ were the same as the initial values, $h_n(0)$. A sum of squares minimization objective function was defined as

$$f = \sum_{n=2}^{N} [h_n(t_v) - h_n(0)]^2 \tag{18}$$

A NAG (1981) quasi-Newton optimization routine was used to obtain the PSS solution. As each function evaluation required the solution of $3N$ differential equations, the computing time was re-

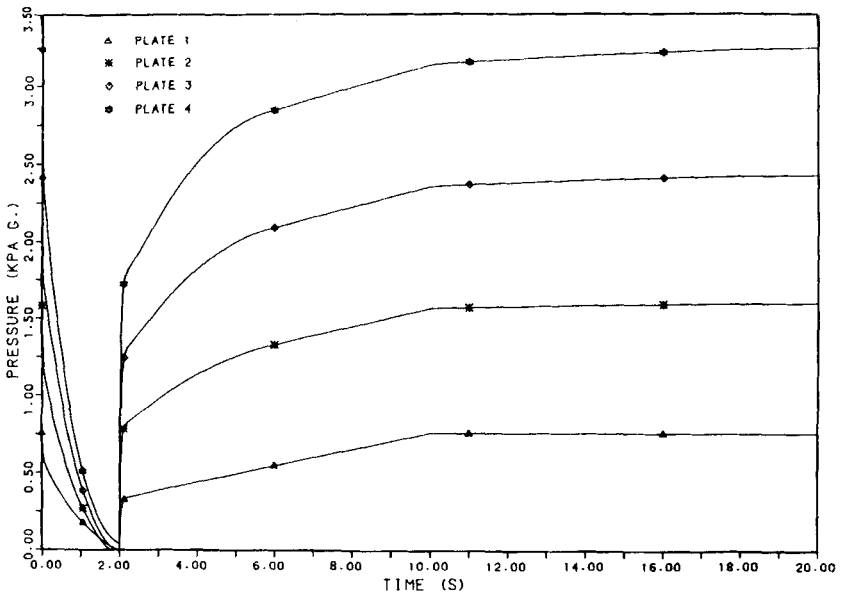

Figure 4. Pressure responses from the hydrodynamic model of a four-plate column.

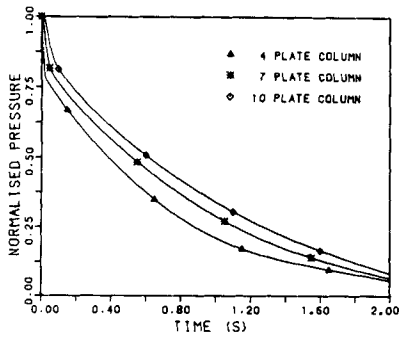

Figure 5. Effect of number of plates on LFP pressure response for the top plate from the hydrodynamic model.

duced by stopping the integration during the VFP, once the liquid had ceased draining. Sequential solution of differential equations, using the holdups at the end of the VFP as the next initial profile was not satisfactory. The convergence was slow and dependent upon the initial estimate due to interactions between the plate holdups and the pressure responses.

The pressure responses obtained from the solution of the hydrodynamic model are shown in Figure 4 for a four-plate column. The column was fitted with a 19 mm vent below the bottom plate and 8 mm vents under the other plates. The negative responses during the LFP are much slower than the 0.06 s obtained from the dry column model due to the effects of the liquid holdup on the vapor flow in the column. The pressure responses consisted of two stages during the VFP, a rapid transient corresponding to the reintroduction of the vapor feed, followed by a slower response as the liquid drained from the TDP and the feed was added to the top plate.

The influence of the number of plates upon the normalized LFP pressure response under the top plate is shown in Figure 5. The pressure transients became more sluggish with an increasing number of plates in the column because of delays in the transmission of the step change resulting from the removal of the vapor feed. The effect of the vent size on the normalized top plate pressure response is shown in Figure 6 for a four-plate column. The initial stage of the response, corresponding to the removal of the vapor feed, was the same for all vent sizes. The remainder of the responses were strongly depend on the vent size as the liquid retards the vapor flow through the plates, forcing the majority of vapor flow to occur through the vents.

The effects of the column parameters on the plate holdups were studied using the PSS solutions of the hydrodynamic model. A typical set of parameter values was selected for a four-plate column with a 19 mm vent under the bottom plate and 8 mm vents below

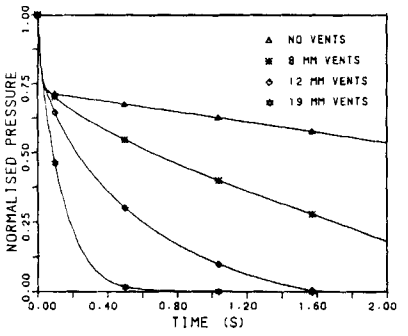

Figure 6. Effect of vent diameter on LFP pressure response for the top plate in a four-plate column.

TABLE 1. SENSITIVITY OF PSS HOLDUPS TO A 10% REDUCTION IN PARAMETER VALUES

Parameter	Holdup Plate 2	Holdup Plate 3	Holdup Plate 4
Standard	83.9 mm	97.0 mm	83.5 mm
	% Deviation From Standard		
Vent Area			
Plate 1	−6.7	−5.6	−7.1
Plate 2	11.1	−7.7	−1.1
Plate 3	−1.7	37.1	−38.2
Plate 4	2.3	−6.4	62.5
Plate Free Area			
Plate 1	−9.9	−10.2	−16.8
Plate 2	12.9	4.0	−1.8
Plate 3	−0.4	13.8	−1.8
Plate 4	0.2	−2.5	15.3
Plate Spacing			
Plate 1	3.5	2.6	3.7
Plate 2	−4.4	2.8	0.4
Plate 3	0.0	−13.5	15.2
Plate 4	−1.1	0.8	−13.1
Vapor Feed Rate	−0.1	−0.4	0.5
Bottoms Discharge Rate	0.2	−1.5	9.1
Resistance to Flow			
Plate Vapor	0.0	−0.2	0.2
Vent Vapor	−1.1	−3.8	−1.0
Plate Liquid	−0.7	−2.1	3.8

the other plates. The results were obtained for a LFP of 2.0 s and a cycle time of 20.0 s. The sensitivity of the standard solution to the parameter values was investigated by reducing each parameter in turn by 10%. The resultant percentage derivations of the PSS holdups on plates 2, 3, and 4 are presented in Table 1. The holdup on plate 1 was externally regulated by the control scheme for the liquid feed addition. Percentage deviations less than 1% were not regarded as significant in view of the accurcy of the solutions.

Variations to the parameters on plate 1 generally had a uniform influence upon the holdups on the plates below because the liquid flow rate from the top plate directly controlled the total mass of liquid added to the column. Reducing the vent area or plate free area slowed the rate of draining and limited the feed addition, which decreased the holdups on the plates below. Conversely, reducing the spacing under the top plate enhanced the liquid flow and increased the holdups.

Variations in the parameter associated with plates 2, 3, and 4 did not produce a uniform effect upon the plate holdups. A reduction in the free area resulted in a substantial increase in the holdups. A reduction in the free area resulted in a substantial increase in the holdup on the plate concerned with only minor changes to the other plates. The effects of a decrease in the vent area was less localized, affecting the adjoining plates. The slower rate of vapor venting retarded the liquid flow from the plate above, increasing the holdup on that plate. The draining from the plate below was enhanced by the slower pressure response above the liquid, resulting in a reduced holdup. Decreasing the vapor space had the opposite effect on the pressure responses and adjoining plate holdups.

The PSS holdup distribution was not significantly affected by variations in the vapor flow rate or the plate resistances to vapor flow. The holdups were not dependent upon the VFP unless appreciable weeping or entrainment occurred.

Hydrodynamic Enthalpy Model

The hydrodynamic enthalpy model was developed to investigate the effect of the latent vapor phase capacity on the hydrodynamic performance of a periodic cycled column. Additional vapor is

generated by flashing of the liquid holdups as the column undergoes the negative pressure transients at the start of the LFP. The isothermal hydrodynamic model as extended to incorporate the effects of enthalpy in a one-component water/steam system. The vapor passing through the plate was considered to totally condense on contact with the liquid. The temperature of the perfectly mixed liquid holdup was assumed to be in equilibrium with the pressure above and the excess enthalpy of condensation resulted in the generation of vapor from the liquid surface. These simplifications were equivalent to assuming a 100% thermal efficiency for the plate.

The hydrodynamic enthalpy model was derived for a column fitted with the TDP and vents to atmosphere under each plate, as shown in Figure 7. The molar balance over the vapor space below plate n becomes

$$\frac{dN_n}{dt} = U_{n+1} - V_n - W_{n,n} \qquad \text{for } n = 1, \ldots, N \tag{19}$$

where U_{n+1} is the vapor generation rate from the holdup on plate $n+1$. Similarly, the molar balance over the liquid holdup on plate n is

$$\frac{dM_n}{dt} = V_n - U_n + Q_{D,n-1} - L_n \qquad \text{for } n = 1, \ldots, N+1 \tag{20}$$

The corresponding enthalpy balance over the late holdup yields

$$C_{P,L}\frac{dM_nT_n}{dt} = V_nH_{V,n} - U_nH_{V,n-1} + Q_{D,n-1}H_{L,n-1} - L_nH_{L,n} \qquad \text{for } n = 1, \ldots, N+1 \tag{21}$$

where H_V and H_L are the vapor and liquid enthalpies. Combining the time derivative of the ideal gas equation with the differentiated vapor volume Eq. 10 gives

$$\frac{dP_n}{dt} = \frac{RT_{n+1}}{dt}\frac{dN_n}{dt} + \frac{P_n}{T_{n+1}}\frac{dT_{n+1}}{dt} + \frac{P_nM_{W,L}}{G_n\rho_L}\left(\frac{dM_{n+1}}{dt} + \frac{dM_{D,n}}{dt}\right) \qquad \text{for } n = 1, \ldots, N \tag{22}$$

The temperature of the liquid of the liquid holdup on plate was described by the differentiated Antoine equation

$$\frac{dT_{n+1}}{dt} = \frac{A_2}{P_n(A_1 - \ln P_n)^2}\frac{dP_n}{dt} \tag{23}$$

An explicit expression for the vapor generation rate U_n can be obtained from Eqs. 19 to 23 as detailed by Thompson (1982). The differential equations describing the pressure responses become

$$\frac{dP_n}{dt} = \frac{P_nT_{n+1}}{G_n}\left[-\frac{K_{1,n+1} + K_{2,n+1}U_{n+1}}{\frac{A_2}{(A_1 - \ln P_n)^2} - T_{n+1}}\right] \qquad \text{for } n = 1, \ldots, N \tag{24}$$

where

$$K_{1,n} = \frac{RT_n}{P_{n-1}}(V_{n-1} + W_{b,n-1}) - \frac{M_{W,L}}{\rho_L}\left(V_n + Q_{D,N-1} - L_n + \frac{dM_{D,n-1}}{dt}\right) \tag{25}$$

and

$$K_{2,n} = \frac{M_{W,L}}{\rho_L} - \frac{RT_n}{P_{n-1}} \tag{26}$$

The plate holdups are described by Eq. 20 and the TDP by Eq. 14.

The initial pressure profile was calculated by iterative methods from the molar holdup distribution with the vapor generation rates determined from an energy balance over the plate. The Gear method from the NAG (1981) subroutine library was the most efficient algorithm for the complete cycle because of the effects of continuous vapor generation from the holdups during the LFP. The hydrodynamic enthalpy model required 15 s of CPU time to solve the differential equations, compared to 3 s for the hydrodynamic model.

The hydrodynamic enthalpy model equations were solved for a water/steam system in a four-plate column fitted with a 19 mm vent under the bottom plate and 8 mm vents below the other plates. The considerable effect of the latent vapor phase capacity in retarding the pressure responses is illustrated in Figure 8 for the vapor space below the bottom plate. The comparative pressure responses were obtained from the hydrodynamic model and the hydrodynamic enthalpy model for the same column parameter and fluid properties. The liquid level on the plate significantly affects the pressure response below plate 3, as shown in Figure 9. The increased holdup generates a greater amount of vapor which retards the pressure response. The slower LFP responses decreases the rate of liquid draining, necessitating a longer LFP which reduces the capacity of the column and causes increased liquid bypassing of the plates. Operating the column with low plate holdups, to minimize these effects, reduces the mass transfer efficiency. The alternative is to remove the vapor rapidly from the columns at the start of the LFP by means of a manifold system.

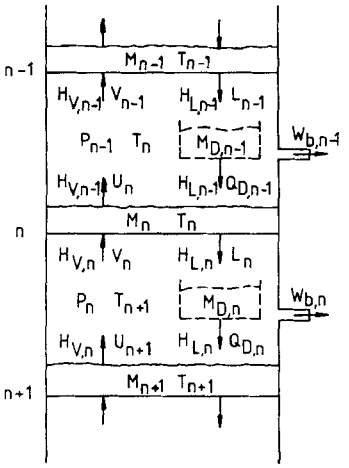

Figure 7. Diagram of column described by the hydrodynamic enthalpy model.

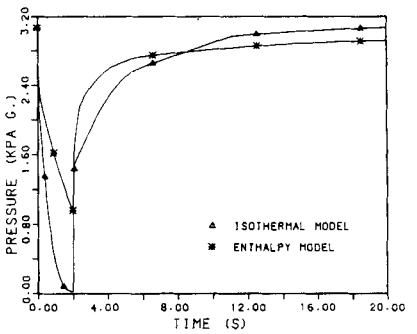

Figure 8. Comparison of isothermal and hydrodynamic enthalpy model pressure responses below plate 4.

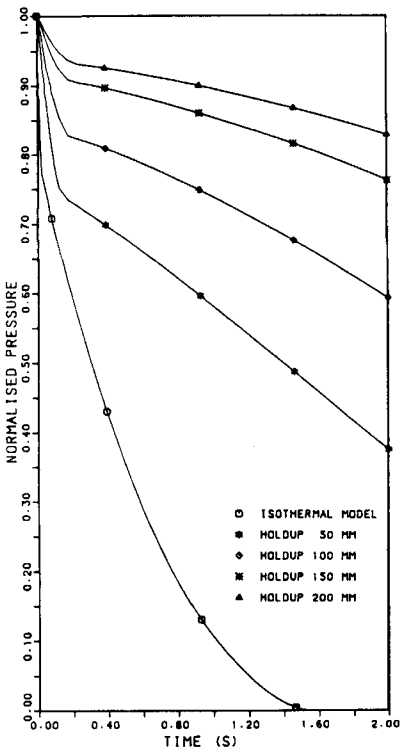

Figure 9. Effect of holdup on the bottom Plate on the LFP pressure response below plate 3.

The effectiveness of four types of manifold arrangements were studied with the hydrodynamic enthalpy model. The simple manifold, with equal branch and manifold diameters, has been used in conjunction with periodic cycled columns when vapor space venting was required. Furzer (1980), using a steady state network analysis, found many of the simple manifold branches had a zero flow. He proposed the exponentially varying area manifold (EVAM) to activate the flows in all branches. The branches areas were determined from the distribution function

$$\left(\frac{A_b}{A_{ct}}\right) = \left(\frac{\bar{A}_b}{A_c}\right) \frac{Ne^{-Di}}{\sum_{i=1}^{N} e^{-Di}} \qquad (27)$$

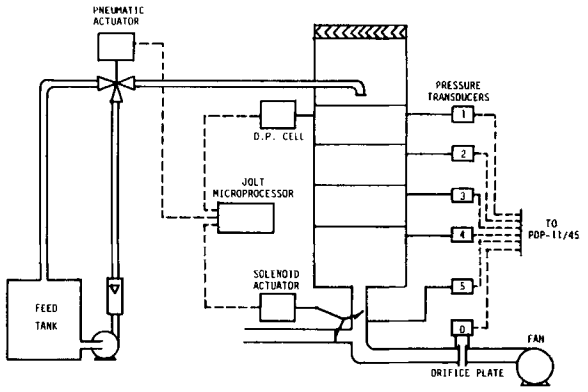

Figure 10. Diagram of experimental equipment.

where D is the model parameter. An extension to the simple manifold is the branch resistance manifold (BRM) which is similar to the vent arrangements used with the hydrodynamic except that they are connected to a common manifold of larger diameter. The pressure in the manifold section is considerably lower than the column and the entire resistance to vapor flow occurs in the branches. The BRM eliminates the flow complexities in the simple manifold and the EVAM.

The major disadvantage of these manifolds is that they operate during the VFP, resulting in a reduction in the efficiency of the column due to vapor bypassing the plates. The original application to a manifold to a periodic cycled column by Robinson and Engel (1966) included solenoid valves in each branch to restrict the venting to the LFP. This method of isolating the manifold during the VFP has limited practicality in large-scale columns. The back pressure manifold (BPM) was designed to provide a simple mechanical isolation of the manifold. It is similar to the BRM with a solenoid-operated valve at the outlet to isolate the manifold during the VFP and a check valve in each branch to prevent vapor bypassing. The branch diameters can be much larger than those used in the BRM, as the manifold only operates during the LFP. The use of check valves to control manifold flows was suggested by Wade et al (1969), but they did not elaborate upon the idea.

The performance of the manifolds was assessed according to the following criteria: i) the percentage of the vapor feed that was vented through the manifold; and ii) η, the fraction of liquid draining from a particular plate, relative to the initial plate holdup.

Table 2. Performance of Manifold Arrangements

Manifold Type	Top Branch Dia. mm	Branch Area Profile	Liquid Flow Period s	Fraction of Liquid Draining, η Plate 1	Plate 2	Plate 3	Plate 4	% Vapor Vented
Simple	10.0	Uniform	2.0	0.028	0.000	0.028	0.101	0.1
Simple	20.0	Uniform	2.0	0.000	0.000	0.000	0.246	2.3
EVAM	10.0	D = 0.1	2.0	0.035	0.000	0.030	0.090	1.2
EVAM	20.0	D = 0.1	2.0	0.137	0.000	0.092	0.239	6.1
BRM	10.0	Uniform	2.0	0.166	0.125	0.070	0.016	8.6
BRM	20.0	Uniform	2.0	0.504	0.373	0.210	0.040	32.9
BRM	10.0	Uniform	4.0	0.448	0.355	0.200	0.131	9.5
BRM	10.0	$\sqrt{2}$ series	2.0	0.318	0.444	0.542	0.467	34.2
BRM	10.0	$\sqrt{2}$ series	4.0	0.782	1.055	1.141	0.962	33.6
BPM	10.0	$\sqrt{2}$ series	2.0	0.236	0.344	0.444	0.405	2.3
BPM	20.0	$\sqrt{2}$ series	2.0	0.560	0.721	0.779	0.690	4.9
BPM	10.0	$\sqrt{2}$ series	4.0	0.667	0.921	1.026	0.854	4.2

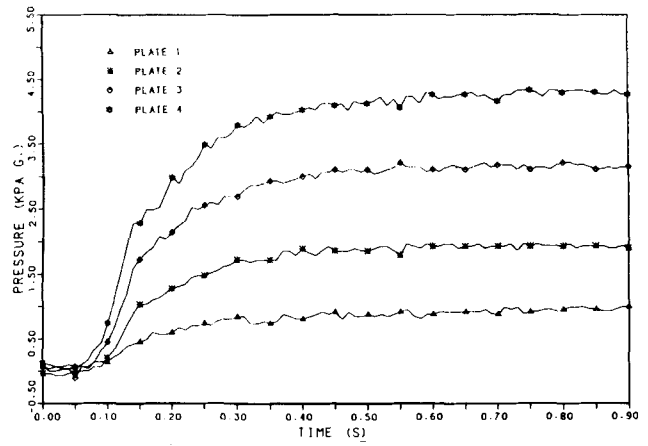

Figure 11. Positive dry column pressure responses after activation of solenoid valve relay.

The performance variables were evaluated by the hydrodynamic enthalpy model during the simulation for the manifolds fitted to a four-plate column with initial plate holdups of 100 mm of liquid. The ideal η was 0.76 for a 2.0 s LFP, assuming instantaneous pressure equalization and no plate mixing, with 3.9 s required for complete plate drainage. A $\sqrt{2}$ series branch area distribution, described by

$$A_{b,n} = 2^{(n-1/2)} A_{b,1} \quad \text{for } n = 1, \ldots, N \tag{28}$$

was used in conjunction with the BRM and BPM. This distribution was based on the theoretical time expression for the venting of a fixed volume and provides equal venting times, assuming a uniform initial pressure profile and neglecting the effects of variations in vapor generation or vapor flow through the plates. The performance of the various manifold arrangements are presented in Table 2.

TABLE 3. COLUMN PARAMETER VALUES

Description	Parameter Value
Plate Area, $A_{c,n}$	
Plate 1	0.292 m^2
Plates 2–4	0.235 m^2
Fraction Plate Free Area, A_f/A_c	
Plates 1–4	0.059
Effective Plate Spacing, $H_{e,n}$	
Below Plates 1–3	0.52 m
Below Plate 4	1.80 m
Plate Resistance to Vapor Flow, $k_{V,n}$	
Plate 1	463
Plate 2	428
Plate 3	431
Plate 4	407
Plate Resistance to Liquid Flow, $k_{L,n}$	
Plates 1–4	525
Vent Resistance to Vapor Flow, k_b	
19 mm vent	1.6
10 mm vent	1.52
8 mm vent	1.59
Residual Pressure Drop, ΔP_R	
Plates 1–4	5 mm water
Liquid Flow Rate	
Feed to Plate 1	1.3 L/s
Bottoms by Pump Only	0.4 L/s
Bottoms with Pump and Drain	0.55 L/s
Time Lags	
Valve Movement	0.16 s
Feed to Plate 1	1.5 s

The commonly used simple manifold with equal branch and manifold areas performed poorly, allowing virtually no liquid flow from the top three plates. The majority of venting occurred from below the bottom plate, which prevented flow from the other vapor spaces. The EVAM, designed to activate flows in the upper branches under steady state conditions, showed no improvement in performance over the simple manifold. The results indicate that the EVAM was not effective when applied to an unsteady state situation.

The BRM eliminated the interaction between the branch flows by incorporating a large-diameter manifold. The results for the uniform branch area profile show poor draining was obtained on the lower plates. Increasing these branch diameters by means of the $\sqrt{2}$ series produced a more uniform η distribution; however, over 30% of the vapor feed was vented. The BPM effectively reduced the vapor loss to less than 5% while maintaining a high uniform η distribution. The BPM, with increasing branch areas down the column, was the most efficient of manifold arrangements studied. It achieved large values of η for a short LFP and maintained acceptable vapor losses. The additional capital cost associated with the BPM is clearly outweighed by the rapid destruction of the pressure profile at the start of the LFP and the corresponding improvements in column performance.

EXPERIMENTAL

A series of experimental studies were performed to measure the dynamic pressure responses and the pseudosteady-state holdup distribution in a periodic cycled column. The results were used to confirm the validity of the hydrodynamic model.

The studies were performed in a four-plate, 610 mm diameter, Perspex column as shown in the schematic diagram, Figure 10. Air, supplied by a 20 kW fan and metered with an orifice plate, was directed to either the column or a bypass line by two 250 mm butterfly valves. The valves were mechanically linked and driven by a 240 V solenoid. The liquid feed was directed onto the top plate by a pneuamtically-activated three-way valve until the pressure set-point below the top plate was reached. The cycle control of the air and liquid feed was performed by a dedicated MOS Technology 6502 Microprocessor, as described by Furzer and Rosolen (1978). The column was fitted with 5.9% free area Perspex sieve plates, and time-delay plates were installed below the top three plates. A 19 nm diameter branch was fitted to each vapor space with the facility for attaching 8 mm and 10 mm diameter restrictions.

The dynamic pressure responses under each plate were measured using

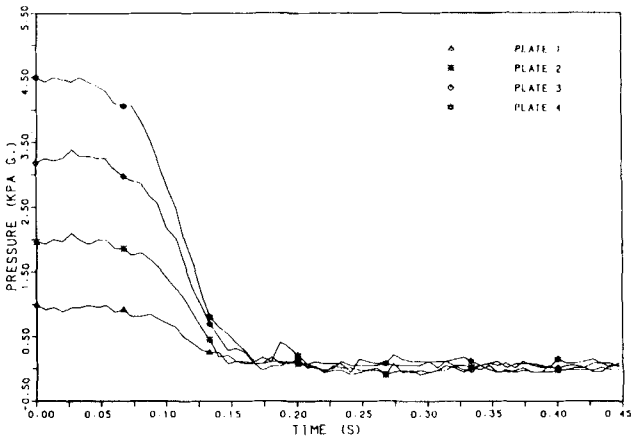

Figure 12. Negative dry column pressure responses after activation of solenoid valve relay.

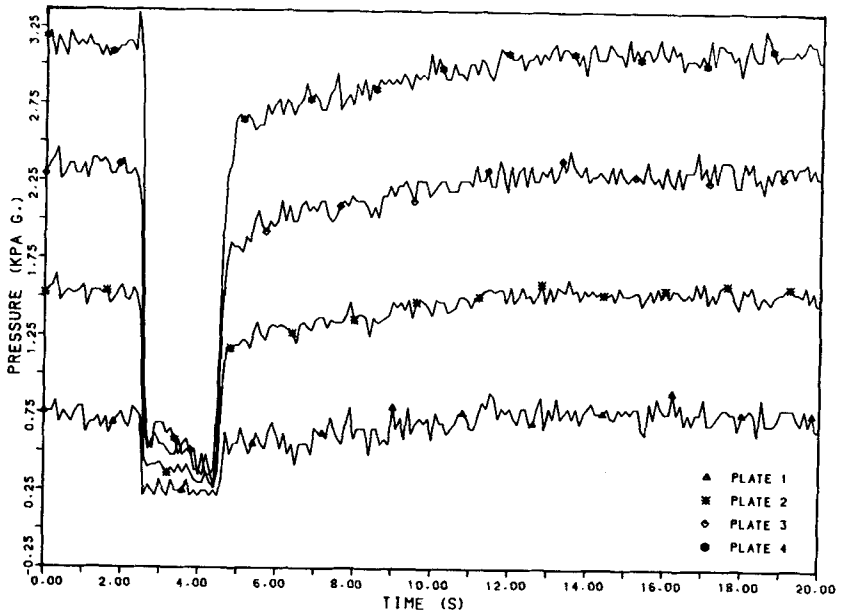

Figure 13. Pressure responses over a cycle from an unvented column.

integrated circuit pressure transducers. Six National Semiconductor LX1701DD differential pressure transducers were installed on the column as shown in Figure 10, and the voltage ouput was logged by a PDP 11/45 computer with real time data acquisition facilities. The vapor valve solenoid relay and the butterfly valve positions were monitored on channels 6 and 7 by logging the voltage the voltage in simple microswitch resistance circuits. Static pressures were measured on a variable inclination manometer.

All the parameters associated with the hydrodynamic model were determined and are summarized in Table 3. The plate resistances to liquid and vapor flow were obtained experimentally from pressure drop and flow measurements. The residual pressure drop was evaluated from the calibration of the wet plate pressure drop to the head of clear liquid on the plate. The lag of 0.16 s in the butterfly valve movement was determined by logging the solenoid relay and valve position circuit voltages on the PDP 11/45.

EXPERIMENTAL STUDIES

Dynamic Experiments

The dry column positive and negative pressure responses are presented in Figures 11 and 12. The results were obtained at an air flow rate of 0.62 kg/s and a data logging rate of 300 Hz. The start of the responses in Figures 11 and 12 corresponds to the change in position of the vapor valve solenoid relay. The initial delay of approximately 0.08 s in the positive responses was due to the time required for the butterfly valve to partially open. The negative responses were extremely rapid, with the majority of the response complete before the 0.16 s valve closure time had elapsed. The rapid dry column responses were dominated by the dynamics of the air supply system.

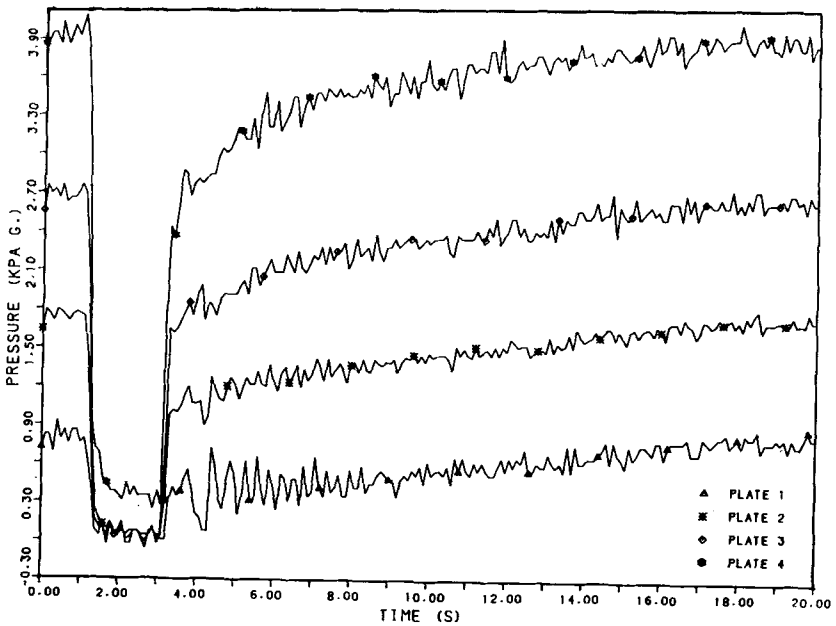

Figure 14. Pressure responses over a cycle from a column with 19 mm vents below each plate.

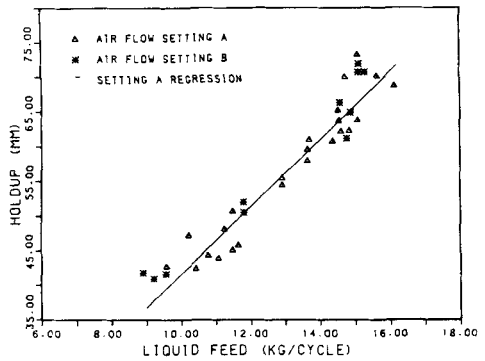

Figure 15. Effect of air flow setting and liquid feed additions on the PSS holdup for plate 3.

The dynamic pressure characteristics of the column with an air/water system are shown in Figure 13, for a complete cycle in an unvented column. The data logging rate was 30 Hz with a total column holdup of liquid of 39 kg. The corresponding responses for a column with 19 mm diameter vents under all plates is shown in Figure 14. The rapid equalization of pressures below plates 1 to 3 during the LFP resulted in enhanced liquid draining and a larger total holdup of 77 kg.

The similarity between the responses at the start of the LFP indicated the vents did not assist the pressure transients corresponding to the removal of vapor feed. During this stage, the mass of vapor flowing up the column was considerably larger than the flow in the vents. The response characterics began to differ appreciably once the liquid holdup on the plates retarded the flow of vapor. In the unvented column, a distinct pressure profile was maintained for the majority of the LFP and the vapor spaces below the plates did not vent completely. The 19 mm vents in Figure 14 quickly destroyed the pressure profile during the LFP and completely vented the vapor spaces below plates 1 to 3. The incomplete venting below the bottom plate was due to vapor leakage across the butterfly valve at the base of the column.

Pseudosteady-State Experiments

The pseudosteady-state plate holdups were calculated from the wet plate and orifice plate pressure drop measurements. The column was operated under a given set of conditions for 50 cycles to allow the column to reach pseudosteady-state. The vents were then closed and the wet plate pressure drops measured on the inclined manometer. The plate holdups were drained into the base where the total column holdup was determined from a calibrated sightglass. The amount of liquid feed added per cycle was measured on the feed tank sightglass.

The liquid holdups on plate 3 for various liquid feed additions is shown in Figure 15, for a column with 8 mm vents under the top three plates and a 19 mm vent below the bottom plate. The results, obtained at two different settings of vapor feed rate, indicated the holdup was independent of vapor flow rate as predicted by the simulations. The plate holdup was linearly dependent upon the liquid feed additions over the range investigated. Similar linear relationships were obtained for the holdups on the other plates. The total column holdup, calculated from the wet plate pressure drops, differed from the measured holdup by less than 4 kg in 93% of the 124 runs conducted under various column conditions.

The trends predicted by the hydrodynamic model compared favorably with those obtained in the experimental studies. Enlarging the vent under plate 3 increased the holdup on plate 4 and reduced the plate 3 holdup. The addition of a 25 mm diameter simple manifold to the column produced results which were similar to the case with a 19 mm vent below the bottom plate and 8 mm vents under the others. The simulations for the simple manifold predicted that the majority of the manifold flow emanated from below the bottom plate, which is an analogous situation to the above vent arrangement. Reducing the length of the LFP produced larger plate holdups because of the shorter time available for draining. Conversely, smaller plate holdups were obtained with long LFP times due to the increased amount of liquid bypassing the plates. Full details of the PSS experimental results are presented by Thompson (1982).

Comparison with Simulation Results

The experimental results were compared to the simulation results

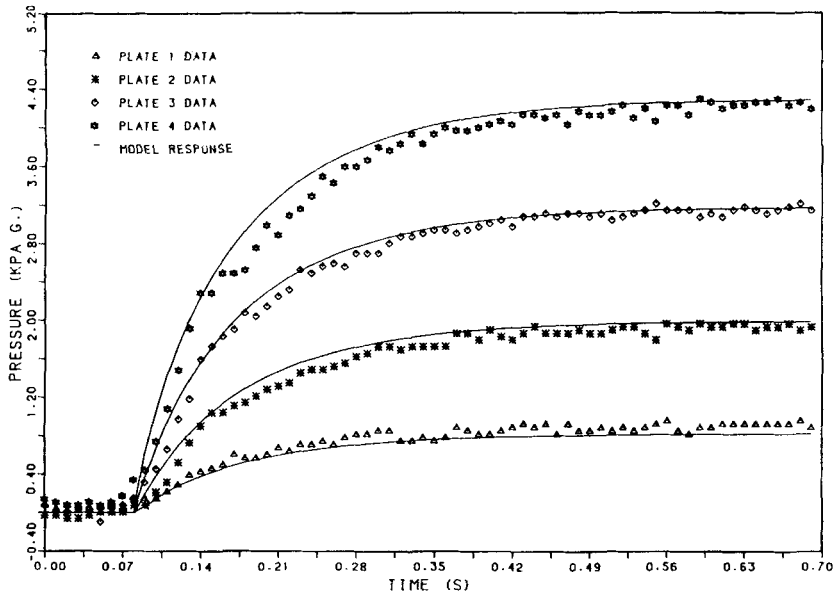

Figure 16. Comparison between experimental positive pressure responses and dry column simulation results.

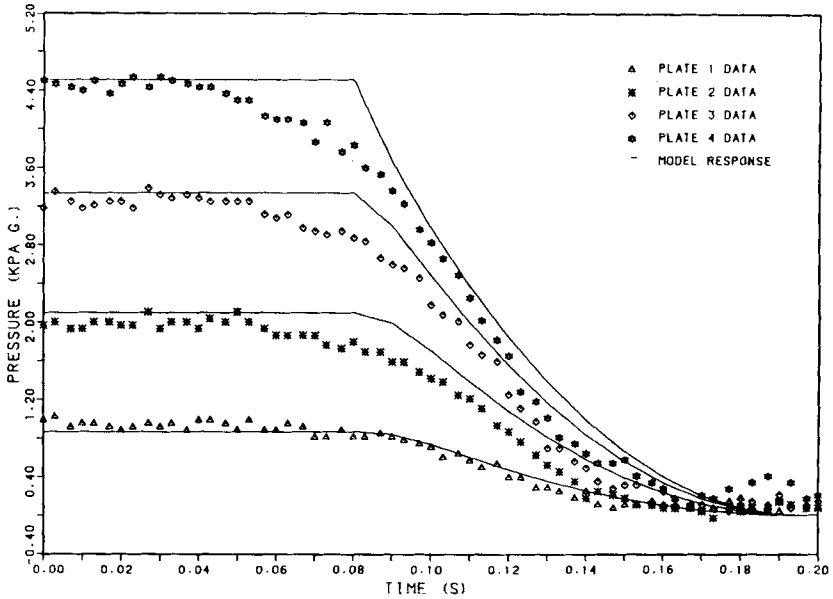

Figure 17. Comparison between experimental negative pressure responses and dry column simulation results.

to evaluate the performance of the models in describing the dynamic and pseudosteady-state hydrodynamic behavior of a periodic cylced column. The comparison between the dry column model and the dynamic results for the positive and negative pressure responses are presented in Figures 16 and 17. A time delay of 0.08 s was included to compensate for the dynamics of the butterfly valve.

The simulation responses compare favorably with the experimental results, with a general deviation of less than 0.2 kPa. The greatest differences occur at the start of the negative response, due to vapor bypassing the column before the 0.08 s had elapsed. The poor flow-regulating capabilities of the butterfly valves and the low resistance to flow in the bypass line, result in very little vapor flow in the column once the valve movement begins. A more sophisticated valve model, involving position-dependent flow resistances and a relation between elapsed time and valve position, would improve the comparison in the initial stages of the response. Overall, the comparisons indicated that the dry column model successfully described the processes occurring.

Two forms of the hydrodynamic model were compared to the dynamic results from a column operating with an air/water system and fitted with a 19 mm vent under the bottom plate and 8 mm vents below the other plates. The standard model was based on the assumption that no vapor flow occurred across the butterfly valve during the LFP. The experimental results indicated some leakage occurred across the valve and a simple, two-parameter orifice plate

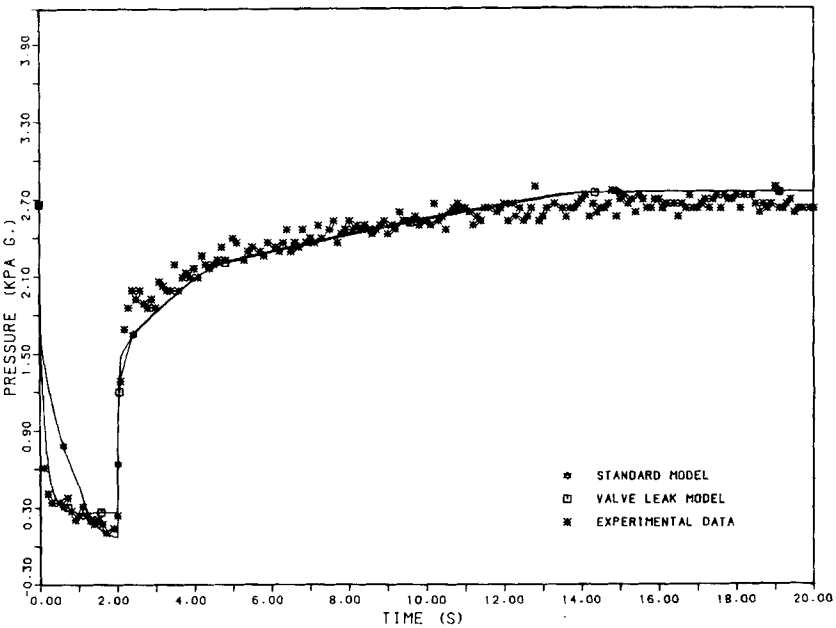

Figure 18. Comparison between experimental pressure response below plate 3 and simulation results.

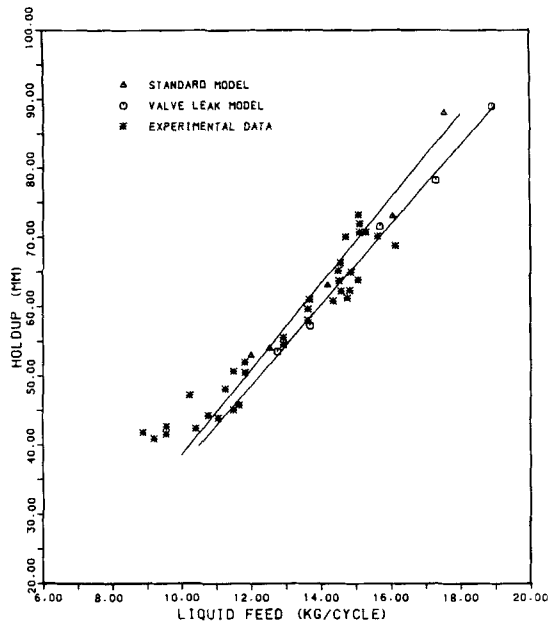

Figure 19. Comparison between experimental PSS holdups on plate 3 and simulation results.

expression was included to describe these effects. The parameters were evaluated from the dynamic data obtained in a number of experimental runs. The comparison between the two forms of the hydrodynamic model and the experimental results for plate 3 is shown in Figure 18.

The hydrodynamic model successfully described the overall dynamic pressure response, with the larger deviations occurring during the LFP. The standard model response was much slower in the initial stages of the LFP, but after approximately 1.0 s had elapsed, the responses compared favorably. The valve leak model followed the pressure transients at the start of the LFP, but was less effective for the remainder of the LFP. A more complex description of the butterfly valve behavior and the dynamics of the air supply system was necessary to fully describe the pressure responses during the LFP. The similarity in pressures at the end of the VFP indicated the differences in responses during the LFP had little effect on the final plate holdup. The introduction of additional parameters would improve the specific comparisons between the column responses and the simulations, but would have limited general applicability.

The pseudosteady-state holdups obtained from the hydrodynamic model are compared to the experimental results for plate 3, in Figure 18. The results confirmed the overall validity of the hydrodynamic model, with the simulation results for all plates falling within 10% of the experimental values. The holdups obtained from the standard model were larger than those predicted by the valve leak model due to the slower dynamic pressure responses in the initial stages of the LFP.

CONCLUSION

The comparison between the experimental results and the simulations confirmed the validity of the models in describing the dynamic and pseudosteady-state performance of periodic cycled columns. A good correlation was obtained between the results and the simulation in view of the model simplifications and the potential uncertainty of some parameters. The sources of deviations in the results were identifiable and attributed to the particular experimental system, rather than inherent weaknesses in the general model.

NOTATION

A_b = branch cross-sectional area, m^2
$\overline{A_b}$ = average branch cross-sectional area, m^2
A_c = column cross-sectional area, m^2
A_1, A_2 = constants in Antoine equation
C_P = molar heat capacity, kJ/kmol · °C
D = parameter in EVAM model
g = acceleration due to gravity, m/s^2
G = vapor volume between plates, m^3
G^* = dimensionless vapor volume
G_T = standard vapor volume between plates, m^3
h = liquid holdup on plate, m
H = molar enthalpy, kJ/kmol
H_e = effective plate spacing, m
k = resistance of plate to fluid flow
k_b = branch resistance to vapor flow
K_1, K_2 = groupings of hydrodynamic enthalpy model parameters
L = molar liquid flow rates from plate, kmol/s
M = molar liquid holdup on plate, kmol
M_D = amount of liquid delayed in vapor space above plate holdup, kmol
M_W = molecular weight, kg/kmol
N = number of plates in column
N_n = amount of vapor between plates, kmol
P = pressure, Pa
P^* = normalized pressure, Pa
P_a = atmospheric pressure, Pa
Q_D = molar flow rate of liquid from TDP, kmol/s
R = universal gas constant, kJ/kmol · K
t = time, s
t^* = dimensionless time
t_v = vapor flow time, s
U = molar vapor generation rate from plate holdup, kmol/s
V = molar vapor flow rate through plate, kmol/s
W_b = molar vapor flow rate in column branch, kmol/s

Greek Letters

α = square root ratio of plate to branch vapor flow resistance
β = ratio of column to branch cross-sectional area
ΔP_d = pressure difference across dry plate, Pa
$\overline{\Delta P_d}$ = average dry plate pressure, Pa
η = fraction of liquid holdup draining from plate during LFP
ρ = denisty, kg/m^3

Subscripts

L = liquid
n = plate number, with top plate defined as 1
V = vapor

Abbreviations

BPM = back pressure manifold
BRM = branch resistance manifold
EVAM = exponentially varying area manifold
LFP = liquid flow period
NAG = Numerical Algorithm Group

PSS = pseudosteady-state
RKM = Runge-Kutta-Merson
TDP = time delay plates
VDP = vapor flow period

LITERATURE CITED

Duffy, G. J., "Periodic Cycling of a Large Diameter Plate Column," Ph.D. Thesis, Univ. Sydney, Australia (1976).

Furzer, I. A., "Periodic Cycling of Plate Columns," *Chem. Eng. Sci.*, **28**, 296 (1973).

——, "Steady State Flow Distributions in a Plate Column Fitted With a Manifold," *Chem. Eng. Sci.*, **35**, 1,291 (1980).

Furzer, I. A., and G. J. Duffy, "Periodic Cycling of Plate Columns: Discrete Residence Time Distribution," *AIChE J.*, **22** (6), 118 (1976).

Furzer, I. A., and K. R. Rosolen, "Microprocessor System for Plate Column Control," *IEEE Trans. IECI.*, **25** (2), 145 (1978.

Gerster, J. A., and H. M. Scull, "Performance of Tray Columns Operated in the Cycling Mode," *AIChE J.*, 16 (1), 108 (1970).

Horn, F. J. M., and R. A. May, "Effect of Mixing on Periodic Countercurrent Processes," *Ind. Eng. Chem. Fund.*, **7** (3), 349 (1968).

Larsen, J., and M. Kümmel, "Hydrodynamic Model for Controlled Cycling in Tray Columns," *Chem. Eng. Sci.*, **34** (4), 455 (1979).

NAG, *Fortran Library Manual, Mark 7*, Numerical Algorithm Group (1978).

Robinson, R. G., and A. J. Engel, "Oxygen Absorption in a Controlled Cycling Apparatus," *Chem. Eng. Prog. Symp. Ser.*, **62** (69), 129 (1966).

Sommerfeld, J. T., et al., "Studies of Controlled Cyclic Distillation. 1: Computer Simulation and the Analogy with Conventional Operation," *Separation Sci.*, **1** (2 & 3), 245 (1966).

Szonyi, L., "Periodic Cycling of Distillation Columns," Ph.D. Thesis, Univ. Sydney, Australia (1981).

Thompson, M. F., "Hydrodynamic Characteristics of Periodically Cycled Plate Columns," Ph.D. Thesis, Univ. Sydney, Australia (1982).

Thompson, M. F., and I. A. Furzer, "Hydrodynamic Modeling for Liquid Holdups in Periodically Cycled Plate Columns," *AIChE J.*, **30**, 496 (1983).

Wade, H. L., C. H. Jones, and T. B. Rooney, "Cyclic Distillation Control," *Chem. Eng. Prog.*, **65** (3), 40 (1969).

Manuscript received Sept. 22, 1983; revision received Oct. 5 and accepted Apr. 30, 1984.